REVISING ESTIMATES OF MARTIAN CRUSTAL HEAT FLOW: IMPLICATIONS FOR BASAL MELTING IN NOACHIAN MARS. K. R. Frizzell[1], L. Ojha[1], and S. Karunatillake[2], [1]Department of Earth and Planetary Sciences, Rutgers University, Piscataway, NJ, 08854, USA, (krf82@eps.rutgers.edu), [2]Lousisiana State University.

Introduction: The planet Mars likely had an active hydrosphere during the Noachian (> 4 Ga) eon, evidenced by the existence of geomorphological features like valley networks [1] as well as the detection of clays and aqueous minerals [2]. However, whether these features indicate surface water or groundwater is a point of contention [3,4]. The Faint Young Sun Paradox (FYSP) calls into question the plausibility of a warm and wet early Mars [5] since climate models struggle to elevate the surface temperatures above the melting point of water for a prolonged period via greenhouse warming alone [6].

This study examines the hypothesis that basal melting of thick ice deposits by geothermal heat during the Noachian was the primary source of liquid water on Mars [4]. On Earth, basal melting is responsible for the formation of subglacial liquid water lakes in various areas of the West Antarctic Ice Sheet [7], Greenland [8], and possibly the Canadian Arctic [9]. Subglacial channels, formed by geothermal heating under the Humboldt glacier in Greenland, even mimic Martian valley networks [8]. Geothermal heating may even be responsible for basal melting of the South polar layered ice deposits on Mars today [10].

After accretion and differentiation, the primary heat source in a planetary interior is from the radioactive decay of heat-producing elements (HPEs) like potassium, thorium, and uranium. With a much higher geothermal heat flow due to the billion-year half-lives of HPEs, basal melting of ice would have been a feasible mechanism for generating liquid water [11]. Therefore, constraining the heat flow on early Mars is vital to climate and geologic models alike, and will aid in understanding the evolution and astrobiological potential of the planet.

Background: We seek to assess whether basal melting from geothermal heat flow is a viable method for sustaining liquid water on Mars during the Noachian eon. Crustal heat flow has been calculated previously by combining elemental abundance maps of Th and K from the Mars Odyssey's Gamma Ray Spectrometer (GRS) with cosmochemical estimates of U and gravity-derived crustal thickness maps [12,13]. These studies hinge on some fundamental chemical and physical assumptions. Our work will vary these assumptions to establish the bounds of the viability of basal melting on Mars [12,7]. We will simulate an array of potential scenarios and create numerous heat flow models of the Martian crust by varying the Th/U ratio, crustal HPE distribution, crustal thickness, and crustal density (see *Table 1*). We will be considering the crustal component of heat flow exclusively for this study.

Methods: We use elemental abundance maps of K and Th derived from PDS-archived GRS spectra projected cylindrically at 5° x 5° resolution. These are representative of the regional regolith chemistry to decimeter depths.

The crustal heat production rate was calculated using the following equation:

$$Q_c = \left[0.9928\, C_U H_{238U} \exp\left(\frac{tln2}{\tau^{\frac{1}{2}}238U}\right) + 0.0071\, C_U H_{235U} \exp\left(\frac{tln2}{\tau^{\frac{1}{2}}235U}\right) + C_{Th} H_{232Th} \exp\left(\frac{tln2}{\tau^{\frac{1}{2}}232Th}\right) + 1.191 \times 10^{-4} C_K H_{40K} \exp\left(\frac{tln2}{\tau^{\frac{1}{2}}40K}\right)\right]$$

where C_x is the concentration of radiogenic elements derived from the GRS chemical maps, H_x is the heat release constants, t is time, and $\tau^{1/2}$ is the half-life of the radioactive elements. The equation was first evaluated at $t = 0$ (present-day) to compare to measurements made by a previous study [12]. The crustal component of heat flow (q_c) is calculated as the product of the crustal heat production (Q_c), crustal density (ρ_{cr}), and crustal thickness (T_{cr}).

Chemical Renormalization: HPE elements may sequester predominantly in primary (igneous) crustal units than secondary (sedimentary) units. Furthermore, sedimentary units where H, Cl, and S may concentrate are only a minor fraction of the crust compared to igneous (extrusive and intrusive) components. Accordingly, as done previously by [13,14], we renormalize each map pixel by:

$$\frac{100}{(100 - w[H_2O] - w[Cl] - w[SO_3])}$$

where w is a mass fraction as a wt%, and the values of $w[SO_3]$ values are stoichiometric mass fractions derived from the S GRS chemical map. We also restrict the analyses to the mid-so-low latitudes, limiting the mass diluting and gamma-spectral effects of H on other elements as described in [15].

Error Analysis: Errors were propagated for the crustal heat production calculation by applying the scalar multiplication and addition equations by Taylor [16]. The GRS maps were the primary source of error, whereas the error on the heat release constants is negligible.

Parameter	Prior Studies	This Work	Supporting Literature
Th/U Ratio	3.8	3 - 4	[12, 17]
Crustal HPE Distribution	Vertically homogeneous	Homogeneous Linear Decrease Exp. Decrease	[12]
Crustal Density	2900 kg/m^3	2500-3100 kg/m^3	[12, 7]

Table 1: Parameters to be varied in this study. Crustal thickness will also be considered based on new data from InSight.

Variation in Th/U ratio: The mass fractions of U are calculated from a cosmochemically constant Th/U ratio of 3.8, as detailed in [12], but recent work shows that the Th/U abundances have been observed to be as low as 3.37 in terrestrial MORB basalts [17]. Therefore, we varied the Th/U ratio from 3 to 4 to see how it impacted crustal heat production during the present-day, which can be seen in both *Fig. 1* and *Fig. 2*.

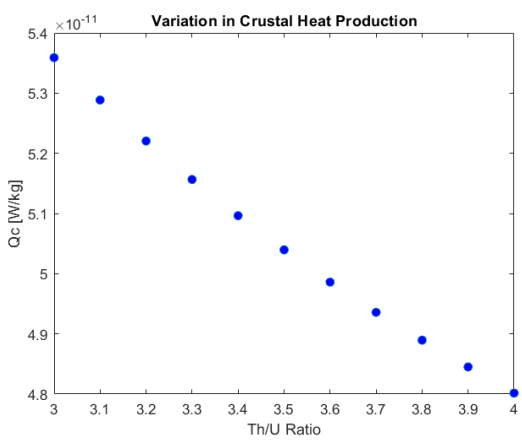

Figure 1: Median crustal heat production in the mid-low latitudes given different Th/U ratios (present-day).

Crustal HPE Distribution: The GRS instrument only measures the top decimeters of the Martian crust, which means the distribution of HPEs at depth is not known. Prior studies [12] have simplified the potential distribution into three regimes: homogeneous distribution, linear decrease, and exponential decrease. Prior work assumes a vertically homogeneous distribution of HPEs in the Martian crust, which is in contrast to the exponential decrease seen in the Earth's crust [18]. This work seeks to analyze all three regimes of crustal HPE distribution in order to constrain potential variations in Martian crustal heat flow.

Crustal Density and Thickness: In order to calculate heat flow, crustal thickness is needed. Crustal density has been estimated from the density of meteorites [19], remote sensing [20], and *in situ* sampling [21], and gravity measurements can be inverted and measured against reference points to get crustal thickness [22]. The emerging understanding of crustal thickness at the InSight seismometer's landing site will also provide a valuable calibration to our data [23]. We therefore intend to explore a wide range of crustal densities in this study (see *Table 1*).

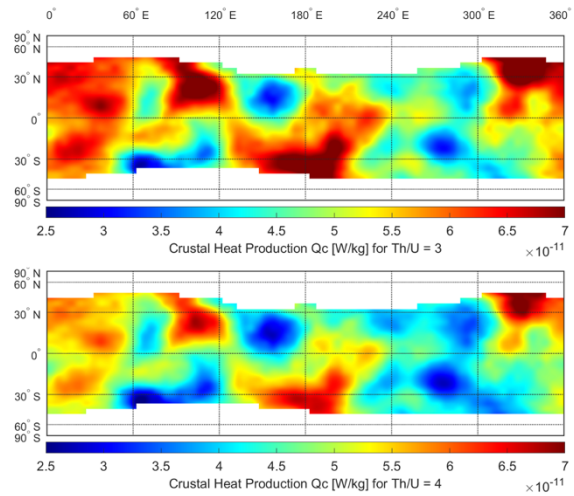

Figure 2: Crustal heat production for Th/U ratios of 3 (above) and 4 (below) evaluated at present-day.

Future Work: Future work will include the generation and analysis of multiple heat flow models based on the variation of the parameters defined in *Table 1*.

Acknowledgments: I would like to acknowledge the Planetary Data System (PDS) for providing the GRS chemical abundance maps, and Rutgers University and my advisor Dr. Ojha for supporting this project.

References: [1] Hynek B. M. et al. (2010) *JGR, 115*, E09880. [2] Ehlmann B. L. and Edwards C. S. (2014) *Annu. Rev. Earth Planet. Sci., 42,* 291-315. [3] Galofre A. G. (2020) *Nat. Geosci.,* 1-6. [4] Ojha L. et al. (2020) *Sci. Adv., 6.* [5] Feulner G. (2012) *Rev. Geophys., 50.* [6] Haberle R. M. et al. (2019) *Geophys. Res. Lett., 46,* 13355-13362. [7] Fisher A. T. et al. (2015) *Sci. Adv. 1(6).* [8] Livingstone S. J. et al. (2017) *Geology*, *45(6)*. [9] Rutishauser A. et al. (2018) *Sci. Adv., 4(4).* [10] Sori M. M. and Bramson A. M. (2019), *Geophys. Res. Lett., 46(3)*. [11] Squyres S. W. and Kasting J. F. (1994) *Science*, *265(5173),* 744-749. [12] Hahn B. C. et al. (2011) *Geophys. Res. Lett. 38*. [13] Taylor, G. J. et al. (2007) *JGR Planets, 112.* [14] Baratoux D. et al. (2014) *JGR Planets, 119.* [15] Boynton W. V. et al. (2007) *JGR, 112(E12).* [16] Taylor J. R. (1982) *An Introduction to Error Analysis, Univ. Sci. Books.* [17] Le Voyer M. (2019) *Geochem., Geophys., Geosys., 20,* 1387-1424. [18] Mareschal J.C. and Jaupart C. (2013) *Tectonophysics, 609,* 524-534. [19] Neumann G. A. et al. (2004) *JGR Planets, 109.* [20] Baratoux D. et al. (2014) *JGR Planets, 119.* [21] Cousin A. et al. (2017) *Icarus, 288,* 265-283. [22] Wieczorek M. A. et al. (2020) *LPSC LI,* Abstract #1393. [23] Knapmeyer-Endrun B. et al. (2021) *Science, 373(6553).*